4. P. Heun, T. Laroche, M. K. Raghuraman, S. M. Gasser, *J. Cell. Biol.* **152**, 385 (2001).
5. C. C. Robinett *et al.*, *J. Cell Biol.* **135**, 1685 (1996); A. F. Straight, A. S. Belmont, C. C. Robinett, A. W. Murray, *Curr. Biol.* **6**, 1599 (1996).
6. W. F. Marshall *et al.*, *Curr. Biol.* **7**, 930 (1997).
7. A. K. Csink, S. Henikoff, *J. Cell Biol.* **143**, 13 (1998).
8. J. Vazquez, A. S. Belmont, J. W. Sedat, *Curr. Biol.* **11**, 1227 (2001).
9. N. Belgareh, V. Doye, *J. Cell Biol.* **136**, 747 (1997).
10. In order to maximize the speed of image capture, we scan one focal section of the nuclear sphere every 1.5 s, and, if necessary, we adjust the objective between scans to keep the GFP-repressor spot in focus. The time required to capture $lac^{op}$ signal is ~15 ms, and the entire nucleus requires <150 ms. We analyse movies in which the plane of focus stays within a 1μm midsection of the nucleus, or roughly half the nuclear depth. To ensure that cell cycle progression is not disturbed as a consequence of light damage, bud emergence and division of the scanned cell are followed by transmission microscopy.
11. Supplementary material is available at www.sciencemag.org/cgi/content/full/294/5549/2181/DC1.
12. P. K. Hanson, J. W. Nichols, *J. Biol. Chem.* **276**, 9861 (2001); P. Heun, S. M. Gasser, data not shown.
13. J. L. DeRisi, V. R. Iyer, P. O. Brown, *Science* **278**, 680 (1997); L. Rubbi *et al.*, *Biochem. J.* **328**, 401 (1997).
14. T. Laroche, P. Heun, S. M. Gasser, unpublished observations.
15. Because the contribution from movement in *z* is not available from our analysis, this is a minimal distance and true velocities cannot be determined.
16. Statistical analysis suggests that sequential vector direction is not entirely random, although tracking shows that movement is not unidirectional. The nature of the constraints are under study (M. Blaszczyk, S. M. Gasser, unpublished observations).
17. A. D. Donaldson, J. V. Kilmartin, *J. Cell Biol.* **132**, 887 (1996).
18. P. Heun, T. Laroche, S. M. Gasser, data not shown.
19. V. Levenson, J. L. Hamlin, *Nucleic Acids Res.* **21**, 3997 (1993); C. Santocanale, J. F. Diffley, *Nature* **395**, 615 (1998).
20. S. Kim, T. A. Weinert, *Yeast* **13**, 735 (1997).
21. S. M. Jazwinski, G. M. Edelman, *J. Biol. Chem.* **259**, 6852 (1984); D. Coverley, R. A. Laskey, *Annu. Rev. Biochem.* **63**, 745 (1994).
22. S. P. Bell, R. Kobayashi, B. Stillman, *Science* **262**, 1844 (1993); M. Foss, F. J. McNally, P. Laurenson, J. Rine, *Science* **262**, 1838 (1993); J. J. Li, I. Herskowitz, *Science* **262**, 1870 (1993); C. Liang, M. Weinreich, B. Stillman, *Cell* **81**, 667 (1995).
23. P. Pasero, D. Braguglia, S. M. Gasser, *Genes Dev.* **11**, 1504 (1997).
24. K. Shimada, S. M. Gasser, unpublished observations. The orc2-1 mutation reduces the number of origins that fire each cell cycle, yet the defect can be suppressed in a dose-dependent manner by overexpressing orc2-1p.
25. Cell-to-cell variability of large movements is aggravated by the irregular shape of orc2 nuclei, which increases error in Metamorph-based distance measurements, based on calculating the center of the nucleus. This variability, however, is not present in trajectory measurements.
26. R. D. Shelby, K. M. Hahn, K. F. Sullivan, *J. Cell Biol.* **135**, 545 (1996); D. Zink *et al.*, *Hum. Genet.* **102**, 241 (1998); E. M. Manders, H. Kimura, P. R. Cook, *J. Cell Biol.* **144**, 813 (1999).
27. P. Buchenau, H. Saumweber, D. J. Arndt-Jovin, *J. Cell Biol.* **137**, 291 (1997); T. Tsukamoto *et al.*, *Nature Cell Biol.* **2**, 871 (2000); T. Tumbar, A. S. Belmont, *Nature Cell Biol.* **3**, 134 (2001).
28. We thank P. Pasero, A. Taddei, and K. Dubrana for comments on the text, F. Neumann for tagging TEL VIR, and the Swiss Institute for Experimental Cancer Research, the Swiss Cancer League, and the Swiss National Science Foundation for support. Boehringer Ingelheim and Roche Research Foundation provided for fellowships to P.H., and IARC to K.S.

14 August 2001; accepted 11 October 2001



# Negative Regulation of Neural Stem/Progenitor Cell Proliferation by the *Pten* Tumor Suppressor Gene in Vivo

**Matthias Groszer,[1,2,4] Rebecca Erickson,[2] Deirdre D. Scripture-Adams,[5] Ralf Lesche,[1,2]* Andreas Trumpp,[7] Jerome A. Zack,[5,6] Harley I. Kornblum,[2,3] Xin Liu,[2,4]† Hong Wu[1,2]†**

**The mechanisms controlling neural stem cell proliferation are poorly understood. Here we demonstrate that the PTEN tumor suppressor plays an important role in regulating neural stem/progenitor cells in vivo and in vitro. Mice lacking PTEN exhibited enlarged, histoarchitecturally abnormal brains, which resulted from increased cell proliferation, decreased cell death, and enlarged cell size. Neurosphere cultures revealed a greater proliferation capacity for tripotent $Pten^{-/-}$ central nervous system stem/progenitor cells, which can be attributed, at least in part, to a shortened cell cycle. However, cell fate commitments of the progenitors were largely undisturbed. Our results suggest that PTEN negatively regulates neural stem cell proliferation.**

The *Pten* tumor suppressor gene encodes the first phosphatase frequently mutated somatically in various human cancers, including glioblastoma (*1*). Besides carcinogenesis, *Pten* may play important roles in brain development, as suggested by its ubiquitous central nervous system (CNS) expression pattern in embryos (*2, 3*) as well as by neurological disorders associated with PTEN germ-line mutations in humans (*4*). However, the early embryonic lethality of conventional $Pten^{-/-}$ mice (*5, 6*) has precluded further studies of PTEN function during brain development.

To explore PTEN's role in early brain development, we generated a conditional *Pten* knockout mouse by flanking exon 5, encoding the phosphatase domain of PTEN, with *loxp* sequences ($Pten^{loxp}$) (Fig. 1A). $Pten^{loxp/loxp}$ females were crossed with males carrying a nestin promoter-driven *Cre* transgene ($Cre^{+/-}$) that is activated in CNS stem/progenitor cells at embryonic day (E) 9 or 10, resulting in almost complete gene deletion in the CNS by midgestation (*7, 8*). In $Pten^{loxp/+};Cre^{+/-}$ mice, *Cre*-mediated deletion of the *loxp* allele (Δ5) was detectable in all neural tissues examined (Fig. 1B, lanes 1 to 5). To ensure complete deletion of *Pten*, we generated $Pten^{loxp/\Delta 5};Cre^{+/-}$ mice carrying a conventional exon 5 deleted allele ($Pten^{\Delta 5}$) and a $Pten^{loxp}$ allele. No PTEN protein could be detected in the mutant brain (Fig. 1C), indicating nearly complete *Pten* deletion. *Pten* deletion leads to hyperphosphorylation of Akt and S6 kinase, known downstream effectors of phosphatidylinositol 3-kinase (Fig. 1C) that have been implicated in neuron survival and cell cycle control (*9*).

Examination of the $Pten^{loxp/\Delta 5};Cre^{+/-}$ brain revealed a marked increase in brain size (Fig. 1D). Measurements taken at E14, E18, and P0 (birth) demonstrated continuous increases in brain weight and in the ratio of brain weight to body weight (Fig. 1E, upper panels). P0 mutant brain weight and cell number were double those of wild-type controls (Fig. 1E, upper and lower left), a difference much greater than that seen in mice overexpressing BCL-2 (*10*) or in mice lacking p27 (*11*). Because deletion of *Drosophila PTEN* led to increased S6 kinase activity and enlarged cell size, we measured the cell size distribution in mutant brains by flow cytometry. Cells from $Pten^{-/-}$ brains were larger than those of controls (Fig. 1E, lower right), providing evidence that PTEN regulates cell size in mammals.

Mutant mice were born with open eyes (Fig. 1D) and died soon after birth. Histological analyses of newborn mutant brains showed a proportional increase in overall brain structures, with no signs of hydrocephalus (Fig. 2A). In the brainstem, nuclei in mutant animals were not easily identifiable (Fig. 2B). It is unclear whether specific nuclei, such as CN7n (arrow), were missing or

[1]Howard Hughes Medical Institute, [2]Department of Molecular and Medical Pharmacology, [3]Department of Pediatrics, [4]Department of Pathology and Laboratory Medicine, [5]Department of Medicine and AIDS Institute, [6]Department of Microbiology and Molecular Genetics, UCLA School of Medicine, Los Angeles, CA 90095, USA. [7]Institut Suisse de Recherche Expérimentale sur le Cancer, Ch. de Boveresses 155, 1066 Epalinges/Lausanne, Switzerland.

*Present address: Epigenomics AG, Kastanienallee 24, 10435 Berlin, Germany.

†To whom correspondence should be addressed. E-mail: xliu@mednet.ucla.edu, hwu@mednet.ucla.edu

disorganized beyond histological recognition. In addition, a severe disturbance of the laminar patterns in the cortex, hippocampus (*12*), and cerebellum was evident (Fig. 2C). Because PTEN controls both cell cycle and cell adhesion or migration, the observed layering defects might be due to uncontrolled progenitor proliferation and/or altered cell adhesion or migration (*13–15*).

We next tested whether *Pten* deletion affected the cell fate determination of neural progenitors. Immunohistochemical analyses of P0 brains were conducted using antibodies specific to the GluR1 subunit of postsynaptic AMPA receptors (Fig. 2D). GluR1 staining was present throughout the brain, indicating that neuronal differentiation had taken place. However, the staining pattern was abnormal, as predicted by the disorganization observed in hematoxylin- and eosin-stained sections (Fig. 2C). To provide more quantitative measurement, we compared the in vitro differentiation potentials of cortical cells from E14.5, the peak of neurogenesis, and E16.5, the onset of gliogenesis. No significant difference between mutant and control was observed in the number of TuJ-1–positive neurons (in green, Fig. 2E) or in the number of glial fibrillary acidic protein (GFAP)–positive astrocytes (Fig. 2F). The degree of induction of astrocyte differentiation in response to leukemia inhibiting factor (LIF) stimulation (*16*) was also not altered by *Pten* deletion (Fig. 2F, right). Thus, the programmed developmental sequence of cell fate determination from neurogenesis to gliogenesis (*17, 18*) is not overtly disturbed by *Pten* deletion. However, neurogenesis is the major event during embryonic brain development, whereas gliogenesis occurs primarily during the postnatal stage (*18, 19*). Thus, we cannot rule out the possibility that postnatally, *Pten* deletion will affect cell fate determination.

To address the mechanism of increased cell number in the mutant, we analyzed progenitor cell proliferation at E14.5 using the nucleotide substitution method. E14.5 was chosen because (i) *Cre*-mediated *Pten* deletion is complete (*12*); (ii) brain weight is not significantly increased relative to control littermates (Fig. 1E), which allowed us to focus on neural stem/progenitor cells rather than more differentiated progenies; and (iii) intensive neural stem/progenitor cell proliferation takes place (*13, 14*). A significant increase in bromodeoxyuridine (BrdU)-labeled nuclei was observed in the ventricular zone (VZ) of mutant animals (Fig. 3, upper panels) (*12*). The increased BrdU labeling in the mutant brain could be due to a shortened cell cycle time (see below), a decrease of apoptosis, or both. Using the TUNEL (terminal deoxynucleotidyl transferase–mediated deoxyuridine triphosphate nick-end labeling) assay (*20*), we were able to detect a significant decrease

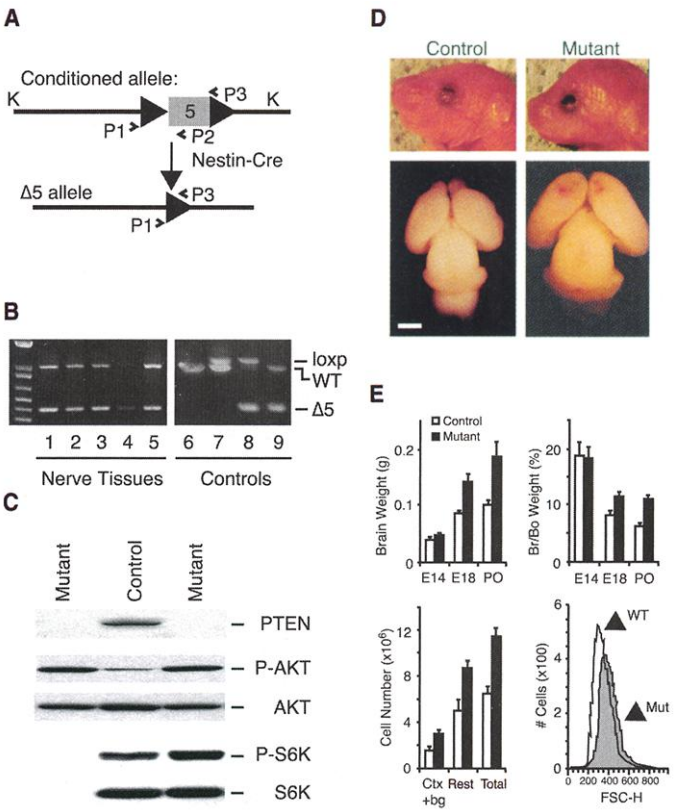


**Fig. 1.** Genotype and phenotype of mice lacking PTEN in the brain. (**A**) Schematic representation of *Pten* conditional knockout allele. P1, P2, and P3 localize polymerase chain reaction (PCR) primers used for genotyping. *Cre*-mediated recombination deletes exon 5 and creates a $Pten^{\Delta 5}$ allele. K, Kpn I site. (**B**) PCR screen for exon 5 deletion in adult $Pten^{loxp/+}$;Nestin-$Cre^{+/-}$ mice. Lanes 1 to 5, DNAs prepared from cortex, hippocampus, cerebellum, spinal cord, and retina, respectively; lanes 6 to 9, DNAs isolated from wild-type (WT), $Pten^{loxp/+}$, $Pten^{loxp/\Delta 5}$, and $Pten^{+}$ mice, respectively. (**C**) Western blot analysis of whole brain lysates from control and $Pten^{loxp/\Delta 5}$;$Cre^{+/-}$ (mutant) newborn mice for PTEN levels, and Akt and S6 kinase phosphorylation using phospho-specific antibodies. (**D**) Macrocephaly (no exencephaly) and open-eye phenotypes in the mutant animals. Scale bar, 3 mm. (**E**) Increased brain weight (upper left and right), cell number (lower left), and cell size (lower right) in mutant mice. Ctx+bg, cortex and striatum; Rest, rest of the brain structures; Total, whole brain. Data are means ± SD; $n = 6$ to 15, $P < 0.01$.

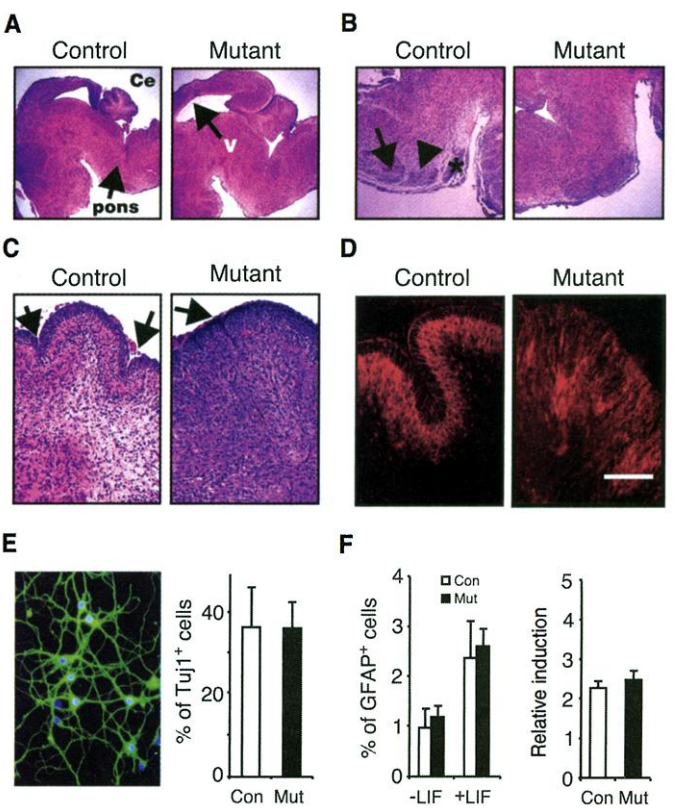


**Fig. 2.** *Pten* deletion causes enlarged, histoarchitecturally abnormal brains. (**A**) Sagittal section shows an increase in overall brain size in mutant animals. V, midbrain vesicle; rostral is to the left. (**B**) Perturbed nuclear structure in the mutant brainstem. Arrow, CN7n facial nerve nucleus; arrowhead, anterior periolivary nuclei; asterisk, pontine gray nucleus; rostral is to the right. (**C**) Disturbed lamination and near-absence of foliation (arrow) of the mutant cerebellum. (**D**) GluR1 immunostaining revealed differentiation despite severely disturbed histoarchitecture. Scale bar, 100 μm. (**E**) In vitro neuronal cultures from E14.5 cortex. (**F**) Cells from E16.5 cortex were cultured for 3 days without or with LIF (50 ng/ml). GFAP-positive astrocytes were counted; data are presented as relative induction in response to LIF stimulation ($n = 4$).

of apoptosis in E14.5 mutant telencephalon (Fig. 3, middle panels) (*12*). Thus, our results indicate that both increased cell proliferation and decreased cell death in the neural stem/progenitor cells probably account for the increased cell number in the mutant animals. We did not observe extensive BrdU labeling in ectopic CNS regions outside the proliferation zone, as has been reported for Rb-deficient mice (*21*). Staining of E14.5 brain sections for the neuronal marker TuJ-1 (in green) showed no sign of disturbed layering and no prominent enlargement of the proliferative zone (dark area) in mutants (Fig. 3, lower panels), as reported for caspase-9–deficient mice (*20*). Taken together, these results suggest that PTEN controls neural stem/progenitor cells by negatively regulating their cell cycle progression rather than preventing postmitotic neurons from reentering the cell cycle. Because nestin is expressed in stem cells and more restricted progenitors in the brain as well as other cell types during development, we cannot rule out the possibility that effects on neural stem cell populations are mediated indirectly by *Pten* deletion in these cell types.

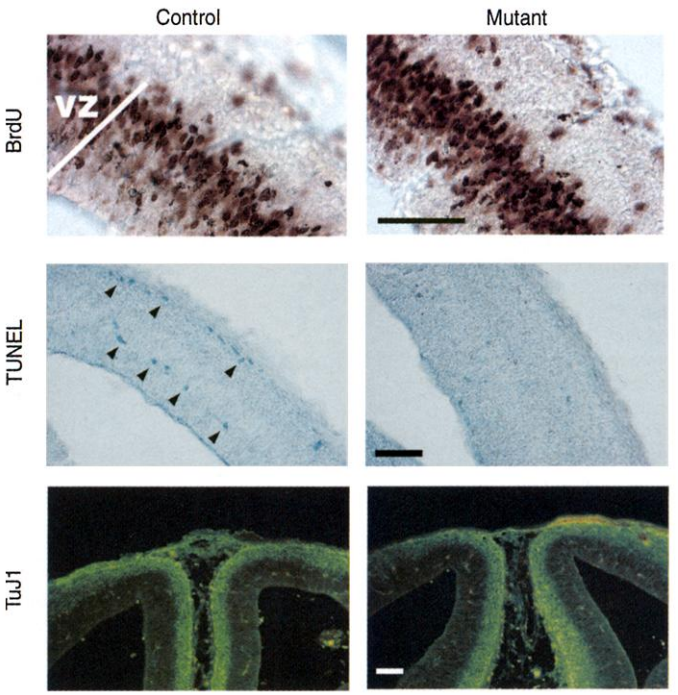


**Fig. 3.** Increased cell proliferation and decreased cell death in the ventricular zone (VZ) of E14.5 mutant telencephalons. Increased numbers of BrdU$^+$ cells (upper panels) but decreased numbers of TUNEL$^+$ cells (middle panels) were observed in mutant cortex. TuJ-1 staining (green) revealed neuronal differentiation (lower panels). Scale bars, 100 μm.

Using the in vitro neurosphere system (*22*), we further studied how PTEN controls neural stem/progenitor cell proliferation. Neurospheres were cultured from E14.5 and P0 (*12*) cortex as described (*19, 23*). Western blot analyses confirmed that no PTEN could be detected in E14.5 neural tissue or in cultured neurospheres (*12*). When cells of E14.5 brains were cultured at moderate density [40,000 cells/ml (*12*)] or clonal density [1000 cells/ml (*12*)], the number of spheres was significantly greater in *Pten* mutants (Fig. 4A), indicating that there were more CNS stem/progenitor cells in mutant animals. Mutant neurospheres propagated more readily, as indicated by a greater average diameter of the spheres (*12*), an increased number of cells per sphere, and a greater number of cells incorporating BrdU (Fig. 4B). Cells in mutant neurosphere cultures were also significantly larger than those in controls (*12*), which suggests that increases in sphere size can be attributed to both in-

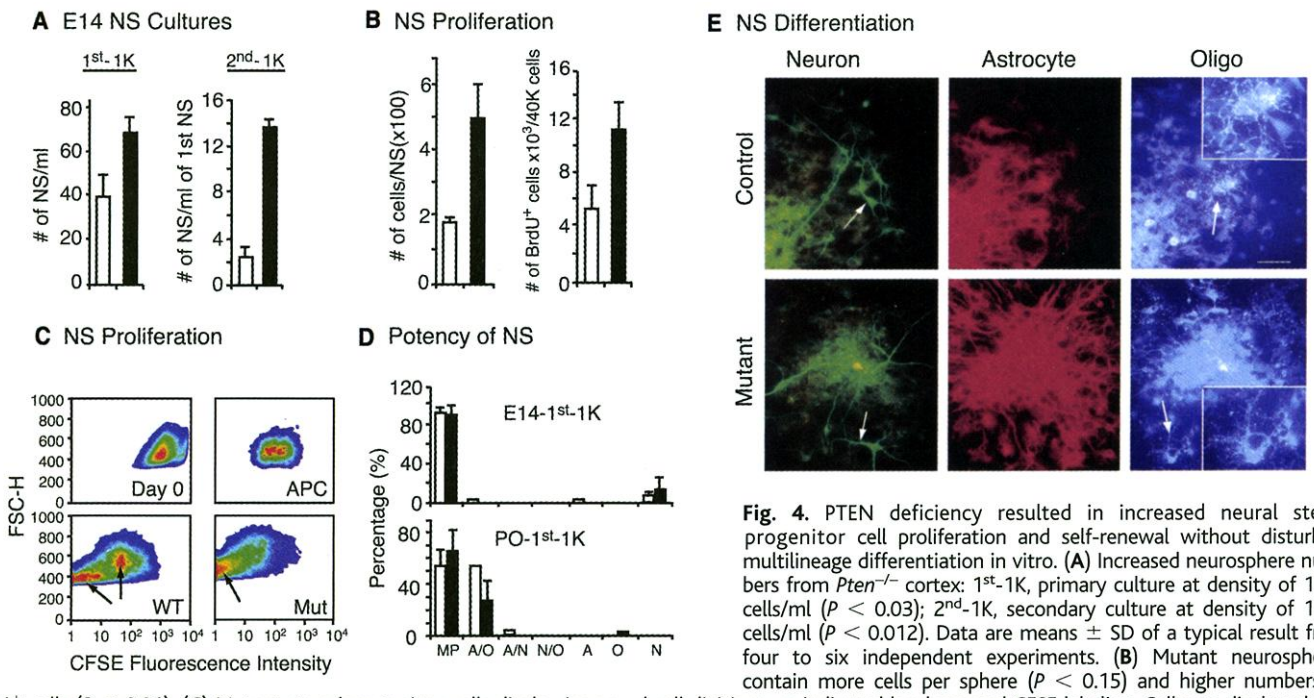


**Fig. 4.** PTEN deficiency resulted in increased neural stem/progenitor cell proliferation and self-renewal without disturbing multilineage differentiation in vitro. (**A**) Increased neurosphere numbers from *Pten*$^{-/-}$ cortex: 1st-1K, primary culture at density of 1000 cells/ml ($P < 0.03$); 2nd-1K, secondary culture at density of 1000 cells/ml ($P < 0.012$). Data are means ± SD of a typical result from four to six independent experiments. (**B**) Mutant neurospheres contain more cells per sphere ($P < 0.15$) and higher numbers of BrdU$^+$ cells ($P < 0.01$). (**C**) Mutant stem/progenitor cells display increased cell divisions, as indicated by decreased CFSE labeling. Cells are displayed in a pseudo-colored density plot, where red represents the highest and blue the lowest cell numbers. APC, aphidicolin-treated. (**D**) Neurosphere potency. Histograms: differentiation potential of E14.5 (upper) and P0 (lower) mutant and control neurospheres cultured at 1000 cells/ml. Data represent three independent experiments. Markers used: αTuJ1 for neurons (N), αGFAP for astrocytes (A), and αO4 for oligodendrocytes (O). MP, multipotent (positive for all three markers). (**E**) A representative of neurosphere differentiation from 2nd-1K cultures. Scale bar, 50 μm. Enlarged photo inserts show oligodendrocytes denoted by the arrows.

creased cell proliferation and enlarged cell size.

To directly test whether PTEN controls cell cycle time, we conducted a CFSE washout experiment. CFSE [5(6)-carboxyfluorescein diacetate succininyl ester] is a fluorescent dye that penetrates cell membranes and is metabolized and trapped within the cell. The dye is evenly distributed to daughter cells, so fluorescence intensity decreases by half with each cell division (*24*). Cells from E14.5 cortex were pulse-labeled with CFSE and cultured in neurosphere medium. After 6 days, neurospheres were dissociated and subjected to flow cytometry. The majority of mutant cells had shifted to the dimmer side of the fluorescence scale, in contrast to wild-type or aphidicolin-arrested control cells (Fig. 4C, arrows), which indicates that most *Pten*$^{-/-}$ cells had progressed through more cell divisions during the same culture period. These studies suggest that PTEN inhibits neural stem cell proliferation in vitro by controlling cell cycle progression.

A key characteristic of stem cells is their self-renewal ability. We compared self-renewal in mutant and control stem/progenitor cells by propagating neurosphere cultures. When neurospheres from primary cultures were dissociated and repropagated at 1000 cells/ml, mutant cultures contained 6.5 times as many spheres per milliliter of the initial culture (Fig. 4A, 2$^{nd}$-1K), a greater difference than for the primary cultures (1$^{st}$-1K); this finding is consistent with the hypothesis that PTEN-null neural stem cells undergo more self-renewing divisions in vitro than do wild-type counterparts. The secondary mutant spheres also proliferated more readily than control spheres, as revealed by their larger diameters (*12*).

Similar to our in vivo studies (Figs. 2 and 3), *Pten* deletion did not alter the differentiation potential of stem cells in neurosphere cultures. Upon differentiation, the spheres from E14.5 and P0 mutant and control animals were generally tripotent, generating neurons, astrocytes, and oligodendrocytes (Fig. 4D); no significant differences in overall sphere potentiality were apparent. The tripotency of clonal secondary spheres was also similar between mutant and control cultures (Fig. 4D). To determine whether *Pten* deletion may affect cell fate specification, we calculated the percentage of neurons within individual spheres. Neurons constituted about 1 to 2%, whereas astrocytes constituted the vast majority of cells present in differentiated neurospheres (Fig. 4E). The percentages of neurons per secondary clonal neurosphere were similar between mutant and controls: 1.54% and 1.34%, respectively.

Taken together, our in vivo and in vitro observations suggest that PTEN negatively controls proliferation of neural stem cells. Caution must be taken in interpreting these results, because a loss of PTEN in neural stem cells may not be responsible for the entire phenotype observed. Our mutant animals are expected to lose PTEN not only in nestin-expressing neural stem cells, but also in all their progeny. Thus, if PTEN is required for normal migration of postmitotic neurons, this effect would be observed in our mutants. Furthermore, nestin is expressed by uncommitted stem cells and committed glial progenitors. Therefore, a direct effect of *Pten* deletion on glial development is not precluded by our results, although an effect on the stem cell population could explain many of our findings. Recent reports indicate that glioblastoma formation in vivo is promoted by transformation of neural progenitor cells, but not differentiated astrocytes, with oncogenic Ras and Akt (*25*). In line with this idea, homozygous loss of PTEN on its own is sufficient to promote proliferation of neural stem/progenitor cells. Thus, this mouse model may help to further understand the biology of this tumor entity.

**References and Notes**


1. J. Li *et al.*, *Science* **275**, 1943 (1997).
2. O. Gimm *et al.*, *Hum. Mol. Genet.* **9**, 1633 (2000).
3. K. Luukko *et al.*, *Mech. Dev.* **83**, 187 (1999).
4. D. J. Marsh *et al.*, *Nature Genet.* **16**, 333 (1997).
5. A. Di Cristofano *et al.*, *Nature Genet.* **19**, 348 (1998).
6. V. Stambolic *et al.*, *Cell* **95**, 29 (1998).
7. B. Bates *et al.*, *Nature Neurosci.* **2**, 115 (1999).
8. G. Fan *et al.*, *J. Neurosci.* **21**, 788 (2001).
9. S. R. Datta, A. Brunet, M. E. Greenberg, *Genes Dev.* **13**, 2905 (1999).
10. J. C. Martinou *et al.*, *Neuron* **13**, 1017 (1994).
11. H. Kiyokawa *et al.*, *Cell* **85**, 721 (1996).
12. For supplemental figures and details of methods, see *Science* Online (www.sciencemag.org/cgi/content/full/1065518/DC1).
13. T. Takahashi *et al.*, *J. Neurosci.* **19**, 10357 (1999).
14. T. Takahashi *et al.*, *J. Neurocytol.* **21**, 185 (1992).
15. J. Liliental *et al.*, *Curr. Biol.* **10**, 401 (2000).
16. A. Bonni *et al.*, *Science* **278**, 477 (1997).
17. S. J. Morrison, *Neuron* **28**, 1 (2000).
18. X. Qian *et al.*, *Neuron* **28**, 69 (2000).
19. V. Tropepe, C. G. Craig, C. M. Morshead, D. van der Kooy, *J. Neurosci.* **17**, 7850 (1997).
20. K. Kuida *et al.*, *Cell* **94**, 325 (1998).
21. E. Y. Lee *et al.*, *Genes Dev.* **8**, 2008 (1994).
22. B. A. Reynolds, S. Weiss, *Science* **255**, 1707 (1992).
23. D. H. Geschwind *et al.*, *Neuron* **29**, 325 (2001).
24. B. F. de St. Groth, *Immunol. Cell Biol.* **77**, 530 (1999).
25. E. C. Holland *et al.*, *Nature Genet.* **25**, 55 (2000).


26. We thank K. Tatsukawa, Y. Wang, and D. Irvin for valuable technical assistance and D. van der Kooy, S. Morrison, H. Herschman, Y. Sun, G. Fan, J. Yuan, and members of our laboratories for helpful comments on the manuscript. H.W. is an Assistant Investigator of the Howard Hughes Medical Institute (HHMI). M.G. is supported by the Swiss National Science Foundation. R.L. was partially supported by HHMI and the Deutsche Forschungsgemeinschaft. Supported by NIH grants NS38489 (X.L.) and MH062800-01 (H.I.K.) and by U.S. Department of Defense grants PC991538 (H.W.) and A136059 (J.A.Z.).

20 August 2001; accepted 11 October 2001
Published online 1 November 2001;
10.1126/science.1065518
Include this information when citing this paper.



**POWERSURGE**

**NEW! *Science* Online's Content Alert Service:** Knowledge is power. If you'd like more of both, there's only one source that delivers instant updates on breaking science news and research findings: *Science*'s Content Alert Service. This free enhancement to your *Science* Online subscription delivers e-mail summaries of the latest news and research articles published weekly in *Science* – ***instantly***. To sign up for the Content Alert service, go to *Science* Online – but make sure your surge protector is working first.

Science
www.sciencemag.org

For more information about Content Alerts go to www.sciencemag.org. Click on Subscription button, then click on Content Alert button.